Jun 29th, 1:30 PM - 3:30 PM

Experimental Study of Head Loss over Laser scanned Rock Tunnel

L. R. Andersson
Lulea University of Technology, robin.andersson@ltu.se

I. A.S. Larsson
Lulea University of Technology

J. G.I. Hellstrom
Lulea University of Technology

P. Andreasson
Lulea University of Technology

A. G. Andersson
Lulea University of Technology

Recommended Citation

Andersson, L., Larsson, I., Hellstrom, J., Andreasson, P., Andersson, A. (2016). Experimental Study of Head Loss over Laser scanned Rock Tunnel. In B. Crookston & B. Tullis (Eds.), Hydraulic Structures and Water System Management. 6th IAHR International Symposium on Hydraulic Structures, Portland, OR, 27-30 June (pp. 22-29). doi:10.15142/T360628160853 (ISBN 978-1-884575-75-4).

6th International Symposium on Hydraulic Structures Portland, Oregon, USA, 27-30 June 2016
Hydraulic Structures and Water System Management
ISBN 978-1-884575-75-4 DOI: 10.15142/T360628160853

Experimental Study of Head Loss over Laser Scanned Rock Tunnel

L.R. Andersson[1], I.A.S. Larsson[1], J.G.I. Hellström[1], P. Andreasson[1,2] and A.G. Andersson[1]
[1]Div. of Fluid & Experimental Mechanics
Luleå University of Technology
Luleå
Sweden
[2]Vattenfall Research and Development
Vattenfall AB
Älvkarleby
Sweden
E-mail: robin.andersson@ltu.se

ABSTRACT

Flow in hydropower tunnels is characterized by a high Reynolds number and often very rough rock walls. Due to the roughness of the walls, the flow in the tunnel is highly disturbed, resulting in large fluctuations of velocity and pressure in both time and space. Erosion problems and even partial collapse of tunnel walls are in some cases believed to be caused by hydraulic jacking from large flow induced pressure fluctuations. The objective of this work is to investigate the effects of the rough walls on the pressure variations in time and space over the rock surfaces. Pressure measurement experiments were performed in a 10 m long Plexiglas tunnel where one of the smooth walls was replaced with a rough surface. The rough surface was created from a down-scaled (1:10) laser scanned wall of a hydraulic tunnel. The differential pressure was measured at the smooth surface between points placed at the start and end of the first four 2 m sections of the channel. 10 gauge pressure sensors where flush mounted on the rough surface; these sensors measure the magnitude and the fluctuations of the pressure on the rough surface. The measurements showed significant spatial variation of the pressure on the surface. For example, sensors placed on protruding roughness elements showed low gauge pressure but high fluctuations. The differential pressure indicated a head loss through the tunnel that was almost four times higher than a theoretical smooth channel.

Keywords: *Pressure measurements, rough surface, hydropower-tunnel, laser scan, friction factor.*

1. INTRODUCTION

Tunnels are often used when transporting water to or from hydropower turbines. In many cases, these tunnels have to be excavated through solid rock, a process which often leads to the occurrence of very large protruding roughness elements on the walls of the tunnels. These roughness elements considerably modify the local cross-sectional area of the tunnel in a more or less stochastic manner. The dynamic action of flow in such tunnels creates disturbances in the flow (Krogstad & Antonia, 1999), (Nakagawa, et al., 2003), (Kruse, et al., 2006) manifesting in, for instance, large pressure variations along the walls of the tunnel; i.e. the rock surfaces are exerted to local net destabilization forces. These forces are likely to contribute to events such as erosion or even partial collapse of the tunnel. These events may, in most applications, be difficult to predict and also hard to detect once they happen. The only indicator of a collapsed tunnel in a hydropower plant may be a substantial drop in turbine efficiency. One method applied with the aim to reduce the destabilizing forces is to "smoothen" the surface and, thus, make it more durable (Barton, et al., 1974); this can be done by spraying concrete on the wall, i.e. shotcreting (Austin & Robins, 1995). The roughness elements of rock tunnels could be considered to be self-similar and random (Perfect, 1997); however, the nature of the roughness elements differ depending on the method used when excavating the tunnel. Rock blasting a tunnel is a rapid method compared to utilizing tunnel boring machines but gives rise to periodic features of the tunnel where large roughness elements of similar size might occur at recurring intervals in the tunnel. These features inhibit the flow, increase the head loss due to friction, and increase the strain on the walls (Andersson, et al., 2012). There might also be new requirements on the tunnels and the operating conditions with the introduction of intermittent energy sources on the market with the demand on the hydropower industry to handle more transient

flow conditions. The purpose of this experiment is to evaluate the pressure fluctuations of a hydro-power tunnel and to determine the effects of wall roughness on the pressure distribution with respect to parameters of wall roughness.

2. EXPERIMENTAL SETUP

The experimental setup consists of a closed-loop water system with a 10 m rectangular Plexiglas channel having one rough surface, a pump, two tanks placed on different levels, and pressure sensors. The high level upstream tank provides a stable driving flow through the tunnel and is connected through a 90° bend with a honeycomb placed at the entrance of the channel to straighten the flow. The honeycomb is 50 mm thick and has a cell diameter of 10 mm. In addition, three guide vanes are mounted inside of the bend to reduce secondary flow effects. The channel is 10 m long to allow the flow to be developed when it reaches the measuring section placed 6 m downstream of the honeycomb. Additionally, the channel is divided into five sections with a height of 200 mm, length of 2000 mm, and a width of 250 mm. The rough surface has an average height of 60 mm and is placed on the left wall in the flow direction of the channel, making the average cross sectional area of each section 250x140 mm^2. The water is collected in the second, downstream tank placed in level with the channel before it is pumped back up to the high-level tank. The flow is controlled with a PID regulator and manual valves and monitored with a flow meter. A schematic of the flow can be seen in Figure 1 where the channel has been mirrored for visual purposes; in the setup, the rough surface is placed on the left wall in the flow direction.

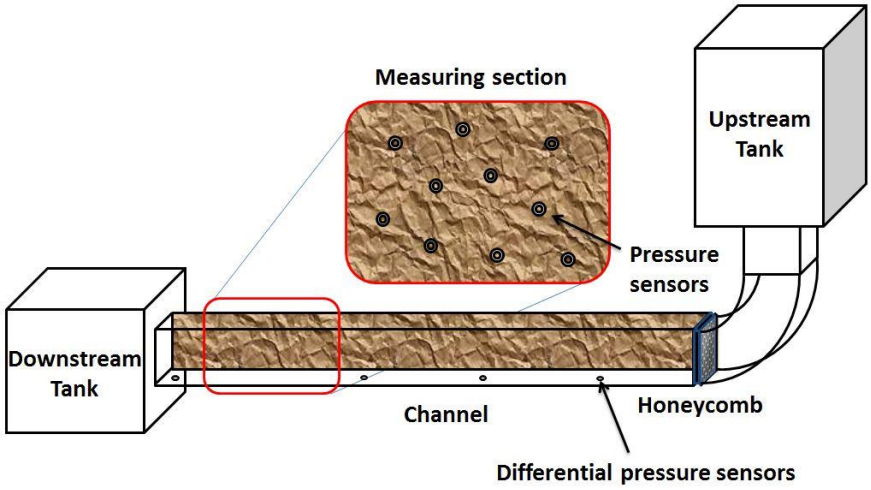

Figure 1. Schematic of the experimental setup used in the campaign, the measuring section started 6 m downstream of the honeycomb, the flow in the figure is from right to left

As mentioned, one sidewall of the tunnel was replaced with a rough surface model (Figure 2). The rough surface is based on a real surface that was captured by a high resolution laser scanning of a rock tunnel, a method that has been proven to be efficient for determining surface roughness (Bråtveit, et al., 2012). The laser scanning was conducted at a resolution of approximately 200 points/m^2. A side wall of the tunnel was extracted and scaled to 1:10 in size; the resulting model is a surface of 250x2000 mm^2 that has an RMS roughness factor of 9.4 mm. The difference between the highest and lowest point on the surface is 56 mm. A right-handed coordinate system is implied throughout this study. The x-axis is directed along the main flow direction with zero at the honeycomb, the y-axis is directed perpendicular to the lower wall pointing upwards, and the z-axis is perpendicular to the rough surface.

Pressure sensors were flush mounted in both the measuring section of the rough surface and every 2 m of the lower channel wall. In the rough surface, the pressure sensors are positioned to represent peaks and valleys of the rough surface (Figure 4). The coordinates for the pressure sensors can be found in

Table 2. The differential pressure sensors were placed on the lower smooth surface on the tunnel. From the differential pressure sensors, it was possible to capture the total head loss over the channel as well as the head loss over specific sections of the channel.

A total of 14 pressure sensors were used in the experiments, 10 pressure sensors in the measuring section and 4 differential pressure sensors. Each differential pressure sensor measures the difference in pressure between two points located at the wall in the inlet and outlet of each of the first four 2 m sections. The pressure sensors used were MTM/N10 104490 from STS, which have a measuring range of 0-10 mwc (meter water column) with an accuracy of ±0.5%. During the experiments, a sampling frequency of 200 Hz was used; all measurements ran between 40-50 minutes and were repeated five times. The magnetic flow meter used was an IFS4000 from Krohne connected to an IFC 110 signal converter. The data acquisition module used in the experiments was a cDAQ-9174 chassis with a Ni9025 module from National Instruments.

Figure 2. The rough surface channel; the pressure gauges can be seen just upstream of the downstream tank

The flow through the channel is pressure driven; the head is adjusted by regulating the water level in the upstream tank placed before the channel inlet (Figure 3), and the water level is regulated by a valve placed under the upstream water tank. The flow rate was regulated by adjusting the pump connected to the loop; the pump was controlled by a PID-regulator (Figure 3), which was connected to a magnetic flow meter. The flow was approximately 63 liters per second ($Re \approx 200\,000$) and differed about ±4% throughout the measured sets.

Figure 3. The upstream water tank and PID-regulator

The upstream water tank was also used when calibrating the pressure sensors. During the calibration, the outlet of the channel was closed and the water level inside of the tank was kept steady at a few different values allowing the pressure sensors to be calibrated. The date and time for each measurement is shown in Table 1, the measurements will follow this denotation throughout the paper.

Table 1. The dates and denotation for each measured set

Date	Denotation
20150602-095023	Set 1
20150602-130400	Set 2
20150602-155523	Set 3
20150603-092302	Set 4
20150603-124918	Set 5

3. RESULTS AND DISCUSSION

The measuring campaign was conducted over two days. All units of pressure are in meter water column [mwc], which will furthermore be denoted as [m]. The head provided by the water tank was kept constant at approximately 3 m. A summary of the measurements can be found in Table 2. The rough surface is placed on one of the side walls of the channel, and, thereby, the height of the pressure sensors differ; this means that the sensors are submitted to different magnitudes of static pressure. These heights can be seen in the sixth column of Table 2. This effect has been adjusted for by subtracting the height of the sensors from the gauge pressure.

Table 2. Summary of the pressure measurements; the third column(σ) is the standard deviation at each point, z denotes the height above or below the mean height of the roughness elements, the chevrons denote the temporal mean

Sensor	Mean Pressure [m]	σ [m]	$<p_{max}\text{-}p_{min}>$ [m]	z [m]	y [m]	x [m]
1	0.3098	0.0295	0.3083	0.0081	0.1210	6.285
2	0.4435	0.0248	0.2410	-0.0049	0.1047	6.490
3	0.2520	0.0272	0.2673	0.0103	0.1828	6.629
4	0.2812	0.0250	0.2399	0.0120	0.0992	6.635

5	0.3352	0.0235	0.2324	-0.0167	0.1598	6.894
6	0.1215	0.0357	0.3676	-0.0005	0.1741	7.060
7	0.4700	0.0225	0.2194	-0.0049	0.0656	7.139
8	0.3262	0.0221	0.2163	-0.0119	0.1551	7.304
9	0.2715	0.0294	0.3028	0.0021	0.1255	7.459
10	0.3121	0.0205	0.1985	-0.0037	0.1427	7.664

3.1. Mean Pressure

In Figure 4, the placement of the pressure sensors on the rough surface are visualized along with one pressure time series. The highest mean pressure can be found in sensors 2, 5, and 7, which are located in valleys on the surface. The high pressure in these zones indicates that there is a loss of velocity in that area due to the sudden decrease of surface elevation, which is to be expected.

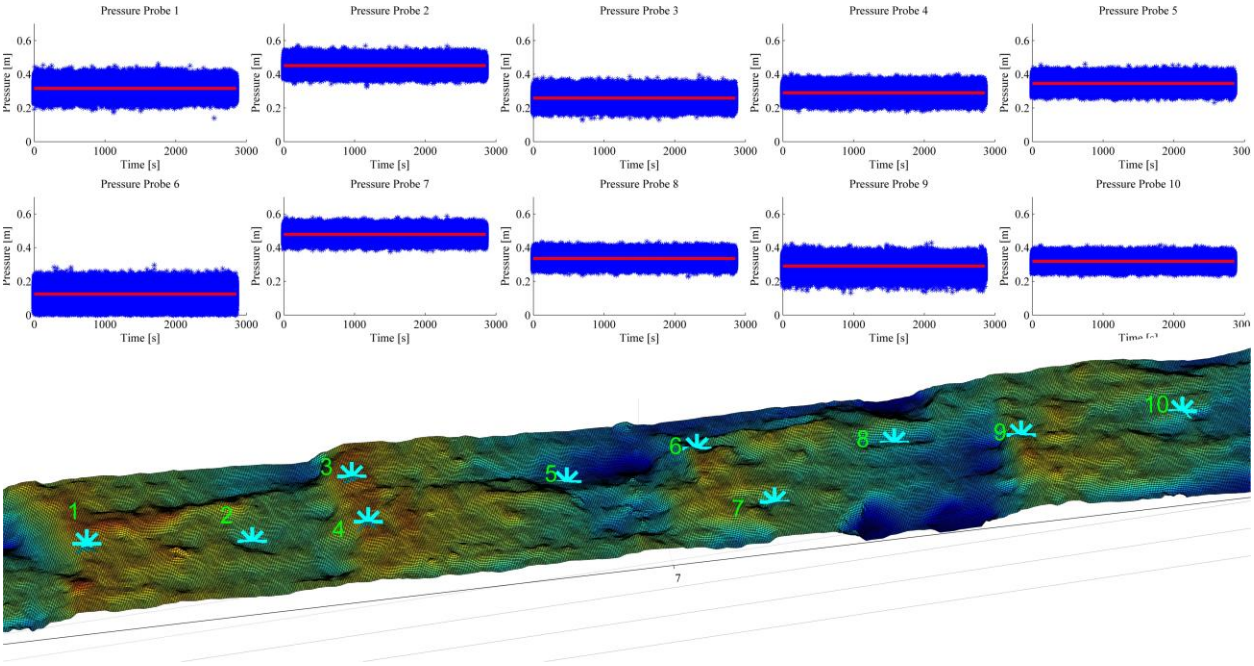

Figure 4. Pressure sensors and the corresponding measured pressure over time, the red lines denotes the average

The results from all five measurements are averaged for each pressure sensor (Figure 5). The figure shows both the amplitudes of the fluctuations and the spread of the averages for each measurement at each point. The difference between each measurement is at most ≈ 10%, which occurs for sensor 9, while the difference for sensor 6 is only ≈ 3%. This shows that the setup in general is insensitive in the sense of reproducing the same conditions during several measurements.

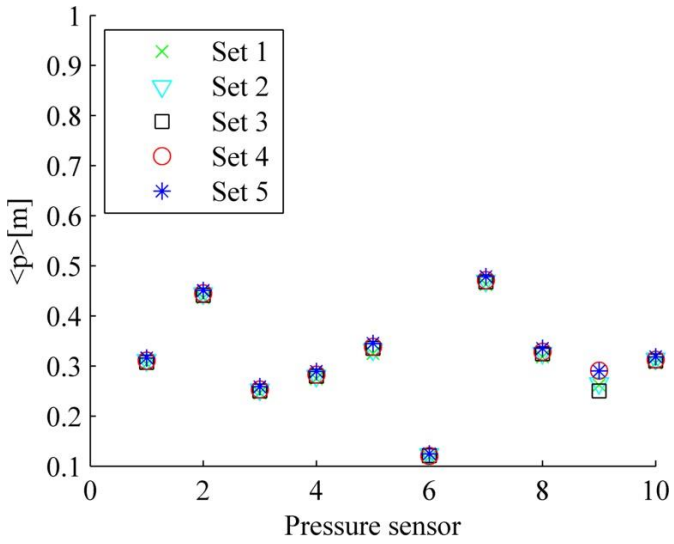

Figure 5. The average pressure in the pressure sensors for all five measurements

The apparent spatial variation in pressure indicates that net forces act on the surface that is not necessarily perpendicular to the main direction of the wall. The largest pressure fluctuations along with the lowest pressure magnitude can be found in position number 6.

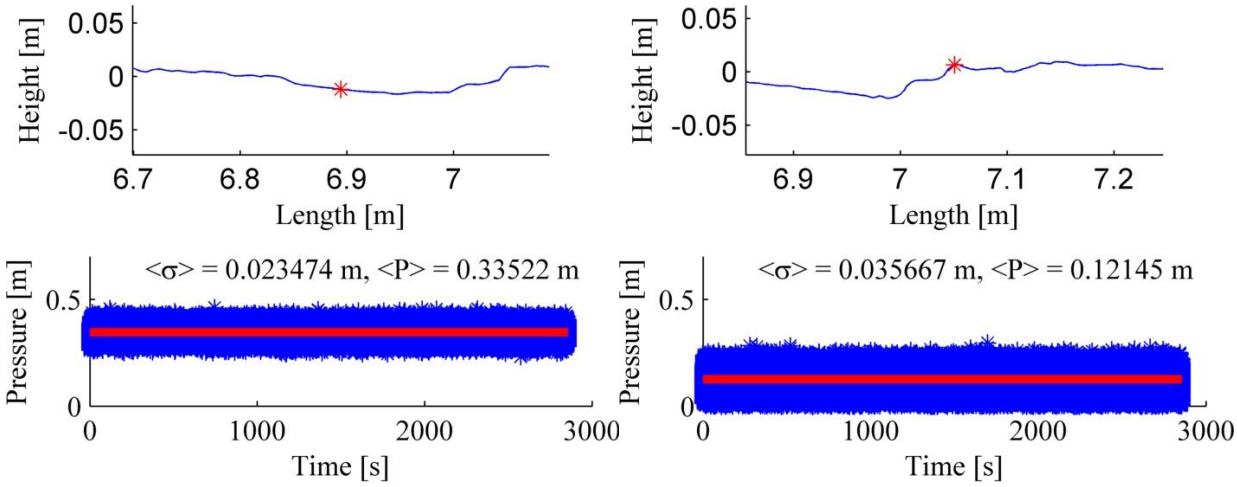

Figure 6. Comparison between pressure point 5 (left) and 6 (right) with the surface profile (top), a measured set (bottom), the standard deviation and the pressure magnitude. The flow goes from left to right.

From Figure 6, it is clear that the gauge pressure is higher in position 5 as compared to position 6. The measurement in sensor 6 shows a higher standard deviation of the pressure than in sensor 5. This can be interpreted as a higher production of turbulence in that position and that there might be some flow separation occurring. Additionally, the distance between these points is merely 166 mm. However, there is evidently a considerable difference in average static pressure and fluctuating pressure. It is not surprising that point 6, which is located on a roughness peak, displays larger fluctuations due to the vorticity generated at the roughness peak; however, the reason for displaying lower average pressure remains to be investigated.

3.2. Differential Pressure

The differential pressure was sampled at the same frequency as the gauge pressure. The differential pressure sensors were placed so that the differential pressure was measured as the difference between the inlet and outlet of each 2 m

section. The total average head loss over the channel is 0.24 m. The measurements from each set of data on each pressure sensor can be found in Figure 7.

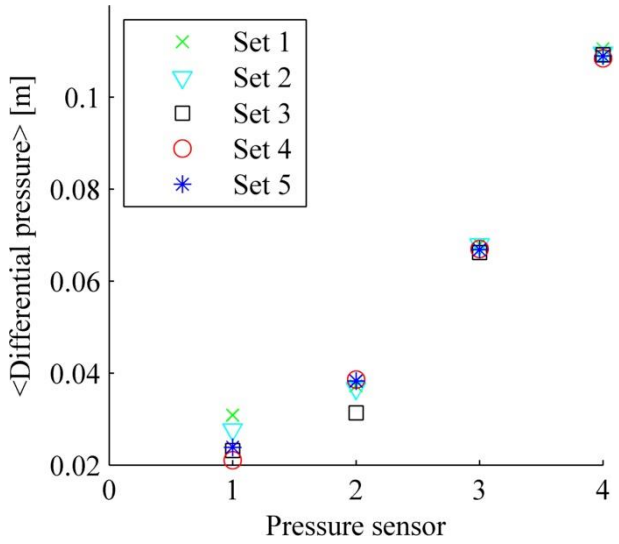

Figure 7. The head loss over the 4 first sections from the entrance of the channel

In the first two sections of the channel, there is some deviation between the differential pressures recorded between the sets; this effect may be due to the valve located under the water tank upstream of the channel. The valve had to be slightly adjusted between the sets and definitely had an impact on the flow at the inlet. However, those discrepancies diminish further downstream in the channel, which points to the conclusion that the perturbations from the valve are small, and the flow is developed in the 4-6 m section and, hence, in the measurement section (6-8 m). One would expect the differential pressure to diminish and approach a constant value through the channel, but instead, the differential pressure seems to increase throughout the channel. The reason for this is unclear, and it needs to be further investigated.

The head loss inside the channel can, to an order of magnitude, be estimated and compared to a theoretical smooth channel by using the Darcy-Weissbach equation (Cengel & Cimbala, 2014):

$$\Delta p = f_d \frac{L\rho}{2}\frac{V^2}{D}, \tag{1}$$

where L is the length of the channel, V is the mean flow velocity, D is the hydraulic diameter of the tunnel, and f_d is the friction factor. We replace D with 4 times the hydraulic radius. The friction factor f_d can be evaluated by using the Colebrook-White equation:

$$\frac{1}{\sqrt{f_d}} = -2\,log\left(2.51\frac{1}{Re\sqrt{f_D}} + \frac{1}{3.7}\frac{k_s}{D}\right), \tag{2}$$

assuming the sand grain roughness factor k_s to be the RMS roughness height of the surface. This is, however, a rough estimate since some of the roughness elements are significantly larger than the RMS value; hence, the flow around the largest roughness elements rather resembles flow around objects than flow over a uniformly rough surface. The results from the estimation can be found in Table 3.

Table 3. The head loss and friction factor for the experiment

	Smooth surface	Measuring section	Darcy-Weissbach
Δp[m]	0.028	0.109	0.139
f[-]	0.015	0.0582	0.0733

The Darcy-Weissbach equation estimates the head loss and the friction factor about 20% higher than the actual measured pressure.

3.3. Conclusions

Pressure measurements of the flow over a rough surface were performed in a downscaled model of a laser-scanned hydraulic tunnel at a Reynolds number of about 200 000. The pressure fluctuations and the wall friction play a crucial role in a number of flow induced effects, such as erosion and hydraulic jacking. These effects are hard to predict, and, therefore, accurate measurements are valuable. The study revealed a range of mean pressures and pressure fluctuations depending on location of the sensor. The largest magnitude of the average pressure was found in the valleys of the rough surface. The largest pressure fluctuations were found in sensors located at peaks of the surface; this can be an effect of vorticity generated at the roughness elements. From the data, it is clear that the pressures in the channel have a very high spatial variance; pressure sensors positioned relatively close to each other displayed different magnitudes and fluctuations of pressure. This indicates that the net forces acting on the rough surface are not uniform and may have a destabilizing effect on sections of the tunnel walls. Decreasing the size of the protruding elements is therefore of interest when excavating rock tunnels. Differential pressure sensors were mounted along the entire length of the channel, enabling measurement of the head loss over the channel. The differential pressure sensors showed a significant increase of the head loss comparing the first and last measured section of the channel. Assuming the RMS roughness height of the surface to be the sand grain roughness factor, the head loss could (to an order of magnitude) be estimated using the Darcy-Weissbach equation. The head loss and the friction factor in the channel is about four times higher than in a theoretical smooth channel with similar dimensions, which indicates that the rough surface has a substantial effect on the flow.

4. ACKNOWLEDGEMENTS

The research presented was carried out as a part of "Swedish Hydropower Centre - SVC". SVC has been established by the Swedish Energy Agency, Elforsk, and Svenska Kraftnät together with Luleå University of Technology, KTH Royal Institute of Technology, Chalmers University of Technology, and Uppsala University. www.svc.nu.

5. REFERENCES

Andersson, A. G., Andreasson, P., Hellström, J. G. I. & Lundström, S. T., 2012. *Modelling and validation of flow over a wall with large surface roughness.* Rome, u.n.

Austin, S. A. & Robins, P. J., 1995. *Sprayed Concrete: Properties, Design and Application.* u.o.:Whittles Publishing.

Barton, N., Lien, R. & Lunde, J., 1974. Engineering Classification of Rock Masses for the Design of Tunnel Support. *Rock Mechanics,* Volym 6, pp. 189-236.

Bråtveit, K., Lia, L. & Bøe Olsen, N. R., 2012. An Efficient Method to Describe the Geometry and the Roughness of an Existing Unlined Hydro Power Tunnel. *Energy Procedia,* pp. 200-206.

Cengel, Y. A. & Cimbala, J. M., 2014. *Fluid Mechanics: Fundemantals and Applications.* 3rd red. u.o.:McGraw-Hill Education.

Krogstad, P. & Antonia, R., 1999. Surface roughness effects in turbulent boundary layers. *Experiments in fluids,* Volym 27, pp. 450-460.

Kruse, N., Kuhn, S. & Von Rohr, P. R., 2006. Wavy wall effects on turbulence production and large scale modes. *Journal of Turbulence,* Volym 7.

Nakagawa, S., Na, Y. & Hanratty, T., 2003. Influence of a wavy boundary on turbulence. I. Highly rough surface. *Experiments in fluids,* Volym 35, pp. 422-436.

Perfect, E., 1997. Fractal Models for the Fragmentation of Rocks and Soilds: A Review. *Engineering geology,* Volym 48, pp. 185-198.